Distinctive Roles for OAS and PKR in the *in Vivo* Anti-Viral Effect of an Adenoviral Vector Expressing Murine IFN-β[1]

Khaldun Al-khatib[*], **Bryan R.G. Williams**[|], **Robert H. Silverman**[|], **William Halford**[#], and **Daniel J.J. Carr**

[*]Department of Ophthalmology, Microbiology, and Immunology, University of Oklahoma Health Sciences Center, Oklahoma City, OK 73104

[|]Department of Cancer Biology/NB40, Lerner Research Institute, The Cleveland Clinic Foundation, Cleveland, Ohio 44195

[#]Tulane University Medical Center, Program in Molecular Pathogenesis and Immunity, New Orleans, LA 70112

Abstract

To evaluate the anti-herpes simplex virus type 1 (HSV-1) mechanisms of murine IFN-β in ocular infection mice were transduced with an adenoviral vector expressing murine IFN-β (Ad:IFN-β). Ocular transduction with Ad:IFN-β resulted in enhanced survival following infection with HSV-1. The protective effect was associated with a reduction in (i) viral titer, (ii) viral gene expression, (iii) IFN-γ levels, and (iv) the percentage of $CD8^+$ T lymphocyte and NK cell infiltration in infected tissue. Expression of IFN-β resulted in an elevation of the IFN-induced anti-viral gene 2′5′-oligoadenylate synthetase (OAS1a) but not double-stranded RNA-dependent protein kinase (PKR) in the cornea and trigeminal ganglion (TG). Mice deficient in the downstream effector molecule of the OAS pathway, RNase L, were no more sensitive to ocular HSV-1 compared to wild type controls in the TG measuring viral titer. However, the efficacy of Ad:IFN-β was transiently lost in the eyes of RNase L mice. By comparison, PKR deficient mice were more susceptible to ocular HSV-1 infection and the anti-viral efficacy following transduction with Ad:IFN-β was significantly diminished in the eye and TG. These results suggest that PKR is central in controlling ocular HSV-1 infection in the absence of exogenous IFN whereas the OAS pathway appears to respond to exogenous IFN contributing to the establishment of an anti-viral environment in a tissue-restricted manner.

Keywords

HSV-1; keratitis; adenoviral vector; IFN-β; OAS; OKR

Introduction

Type I IFNs, IFN-α and -β (IFN-α/β) are multifunctional cytokines released from almost all cells in the body in response to viral infection. The synthesis of proteins involved in intracellular resistance against virus replication include 2′, 5′ –oligoadenylate synthetases (OAS)[2] and double-stranded RNA-dependent protein kinase R (PKR). OAS are a group of enzymes that catalyze the synthesis of 5′ –triphosphorylated, 2′ to 5′ linked oligoadenylates, typically three or four nucleotides in length (1). These molecules bind with high affinity to RNase L, an endoribonuclease that catalyzes the cleavage of single-stranded mRNA and rRNA, thereby leading to inhibition of protein synthesis (2). Relative to HSV-1 infection, disruption of the RNase L gene does not increase the susceptibility of primary murine TG cultures to HSV-1 replication (3). PKR is a serine/threonine kinase that is normally inactive, but is activated by binding to dsRNA or other polyanions (4,5). Activated PKR suppresses translation initiation via phosphorylation of eukaryotic initiation factor 2 (6) and acts as a signal transducer for proinflammatory gene expression (7). Studies have demonstrated the absence of PKR greatly increases HSV-1 replication in mouse cell lines (8,9), primary TG cultures (3), and mice (10).

In addition to inducing cellular genes that confer resistance against viral replication, type I IFNs also influence the direction of the ensuing innate and adaptive immune response to the viral pathogen. NK cells, shown to be involved in suppressing HSV-1 replication (11), are activated in response to type I IFN with enhanced cytolytic activity and proliferation (12). IFN-α/β also can activate dendritic cells (DC) (13) resulting in the production of IL-15 (14) which can augment NK cell activity (15) resulting in suppression of HSV-1 replication (16). The activation of DC by type I IFN also leads to expression of CXCL10 (17), a potent chemokine that has recently been shown to be a central component in ocular HSV-1 inflammation (18). Finally, IFN-α/β have the potential to indirectly influence adaptive immune responses by driving the maturation of DC type 1 to promote a T_H1 response versus a T_H2 response (19).

Although type I IFN are a critical component in the host's repertoire against ocular HSV-1 infection (20), NK cells (21), PMNs (22), macrophages (23), and CD4^{+} T lymphocytes (24,25) have all been found to significantly contribute to the clearance of the virus within the eye. These effector cells either directly lyse virally-infected cells through cytolytic activity (e.g., NK cells) or alternatively, secret cytokines including IFN-γ (26) that either alone or synergistically with locally produced type I IFN block HSV-1 replication (27, 28).

In this study, the feasibility of using a recombinant adenovirus vector to successfully transduce the corneal epithelium with murine IFN-β was examined in HSV-1-infected mice. IFN-β was chosen because among members of type I IFN, IFN-β was shown to be the most efficacious in inhibiting HSV-1 replication *in vitro* (29). Other beneficial aspects of IFN-β are worth considering as well. Specifically, IFN-β is not only a potent anti-viral cytokine but

---

[2]Abbreviations used in this paper: OAS, 2′, 5′ –oligoadenylate synthetases; PKR, double-stranded RNA-dependent protein kinase R; TG, trigeminal ganglia; DC, dendritic cells; Ad, adenovirus vector; GFP, green fluorescent protein; p.t., post transduction; p.i., post infection; MOI, multiplicity of infection; CPE, cytopathic effect; NSE, neuron-specific enolase; PFU, plaque forming units; ICP27, infected cell protein 27; TK, thymidine kinase; VP16, virion protein 16; EMCV, encephalomyocarditis

possesses anti-inflammatory traits as well (30,31). Since acute ocular HSV-1 infection results in an impressive inflammatory response in the murine host (32,33) resulting in tissue pathology and corneal opacity ultimately affecting visual acuity, the combined anti-inflammatory and anti-viral properties of IFN-β are advantageous when considering a highly sensitive and structurally organized tissue such as the eye.

Materials and Methods

Mice, cells, and virus

Female 8–12 week old ICR mice (Harlan-Spargue Dawley, Indianapolis, Ind.) as well as C57BL/6 mice (Jackson Labs, Bar Harbor, ME), RNase L-null mice (34), and PKR-null mice (35) were used in these experiments. Both RNase L-null and PKR-null mice are on a C57BL/6 background. All animals were handled in accordance with the National Institutes of Health guidelines on the care and use of laboratory animals (Publication no. 85–23, revised 1996). All procedures were approved by the University of Oklahoma Health Sciences Center institutional animal care and use committee. L929 and Vero cells were obtained from the American type culture collection (ATCC, Manassas, VA) and propagated in DMEM or RPMI-1640 medium respectively, containing 0.375% HCO_3 supplemented with 10% FBS and antibiotic/antimycotic solution (GIBCO, Gaithersburg, MD) (referred to as complete DMEM or RPMI respectively)

The viruses used in this study were McKrae strain of HSV-1 and vesicular stomatits virus (VSV) (a gift from Dr. Robert Fleischmann, UTMB). HSV-1 and VSV were propagated in Vero cells and aliquots were stored at −80 °C. Three replication-defective adenoviral vectors (ΔE1–ΔE3) were used in this study: Ad:GFP (green fluorescent protein), Ad:IFN-β, and Ad:Null (empty vector). The adenovirus vectors were constructed as previously described (9). The adenoviral vectors were all propagated in E293 cells (ATCC) and the E1-complementing cell line under the following conditions: complete DMEM, 37° C, 5% CO_2, and 95% humidity.

Establishment of TG cell cultures

TG cell cultures were prepared as previously described (3). Briefly, TGs were aseptically removed from mice and treated with a cocktail of collagenase type IV and XI (1 mg/ml; sigma) at 37° C for 75 to 90 minutes. Following dissociation, cells were washed and plated on cover slips coated with laminin and collagen. Cultures were incubated in a 37 °C tissue culture incubator (5 % CO_2, 95% humidity).

Immunocytochemistry

Seven days after the establishment of cultures on cover slips, cells were fixed for 30 min in 3 % paraformaldehyde in PBS containing 0.1 % Triton X (pH 7.5) and then rinsed three times with 1.0 ml of PBS/0.1 % Triton X (pH 7.5). Nonspecific binding sites were blocked using 10 % normal horse serum for 30 minutes. Cells were incubated overnight with polyclonal rabbit anti-neuron-specific enolase antibody (NSE) (Chemicon, Temecula, CA) (1:100 dilution) and mouse anti-GFP antibody (Molecular Probes, Eugene, Oregon) (1:250 dilution) in PBS (pH 7.5) containing 10 % normal horse serum and then rinsed three times

with 1.0 ml of the same buffer. Subsequently, the cells were incubated with Texas red-conjugated goat anti-rabbit IgG (Vector Laboratories, Burlingame, CA) (1:200 dilution) and alexafluor 488–conjugated goat anti-mouse IgG (Molecular Probes, Eugene, Oregon) (1:100 dilution) in PBS (pH 7.5) for 1 hr and washed three times for 5 min each with PBS (pH 7.5). Subsequently cells were mounted and nuclei were counterstained with DAPI (Vector Laboratories, Burlingame, CA). The cells were subsequently viewed using a Nikon E800 fluorescent microscope. Cells treated without primary antibodies served as controls.

Animal studies

Mice were anesthetized with ketamine (100 mg/kg of body weight) and xylazine (10 mg/kg) in PBS administered intramuscularly. Following scarification of the cornea, 1×10^6 transducing units of either Ad:IFN-β or Ad:Null was topically applied to the eye in a volume of 5 ul of PBS. Twenty-four hr prior to, at the time of, or at various time points post transduction (p.t.), mice were anesthetized and infected with HSV-1/McKrae strain (150 pfu/eye for ICR mice and 600 pfu/eye for C57BL/6 wild type and knockout mice). For survival studies, mice were monitored over 30 days post infection (p.i.) and mortality was recorded for each group of animals. For viral titers and viral gene expression, mice were euthanized and corneas and TGs were extracted and subsequently processed as described below.

Determination of IFN-β concentration

Transduced corneas *in vivo* were excised and placed in complete DMEM media 48 hr p.t. Forty eight- hours later, the cornea and the incubating media were placed in 2-ml tubes and homogenized. Homogenates were clarified by centrifugation (10,000×g, 6 min). L929 cells were incubated for 24 hrs with serial dilutions of supernatants and subsequently infected with VSV at a multiplicity of infection (MOI) = 0.05. When the cytopathic effect in the control wells was maximal (between 32–36 hrs p.i.), plates were stained with crystal violet. In each assay, standards with recombinant murine IFN-β (PBL Biomedical Laboratories, New Brunswick, NJ) were employed. The standards themselves were calibrated against WHO international standard IFN-β (Braton Biotech, Inc., Gaithersburg, MD). Fifty percent inhibition of cytopathic effect (CPE) was equivalent to 1 IU/ml for IFN-β. Therefore, the inverse of the dilution of each sample that inhibited 50% CPE was defined as the concentration (in units/ml) of biologically active IFN.

Measurement of viral titers

Following extraction, corneas and TGs were homogenized and freeze-thawed once. The homogenates were clarified by centrifugation (10,000×g, 6 min). Supernatants were then serially diluted and placed (100 μl) onto Vero cell monolayers in 96-well culture plates. After 1-hour incubation at 37° C in 5% CO_2 and 95% humidity, the supernatants were discarded, and 100 μl of an overlay solution (0.5% methylcellulose in culture medium) was added on top of the monolayers. The cultures were incubated at 37° C in 5% CO_2 and 95% humidity for 36–48 hours to observe plaque formation, and the amount of infectious virus was reported as plaque forming units (pfu)/cornea or pfu/TG.

IFN-γ ELISA

To quantitate the content of IFN-γ protein at day 7 p.i., isolated TGs were briefly homogenized and treated with a lysis buffer supplemented with a cocktail of EDTA-free protease inhibitors (CalBiochem, La Jolla, CA). Samples were then centrifuged and supernatants were assayed in triplicate using an enzyme-linked immunosorbent assay (ELISA) specific for mouse IFN-γ (R&D, Minneapolis, MN). The ELISA was carried out according to the manufacturer's protocol and analyzed at an absorbance of 450 nm using a FL600 microplate fluorescence reader (Bio-Tek Instruments, Inc., Winooski, VT). Correlation coefficients consistently were above .9900 and variation between assays was less than 5%.

Flow cytometry

TGs were extracted and treated with collagenase for 90 minutes. Single cell suspensions of TG were pooled and passed through a 40 micron filter. Aliquots of TG cells (1 TG equivalent) were added to 5 ml polystyrene round-bottom tubes (Becton Dickinson, Franklin Lakes, NJ) and stained for cell surface markers. Single cell suspensions of TG were stained with anti-CD16 and subsequently stained with the PE-conjugated anti-CD4, anti-CD8α, anti-DX5, and FITC conjugated anti-CD3 antibodies for 30 min at 4°C followed by two washes ($500 \times g$, 5 min). The cells were then fixed in 1% paraformaldehyde (PFA, Electron Microscopy Sciences, Fort Washington, PA) and stored at 4°C until analysis (18–24 hr later). The cells were analyzed on a FACSCalibur (Becton Dickinson) using WinMDI data analysis software.

Reverse transcription

Cornea and TGs were excised and RNA was extracted in Ultraspect RNA isolation reagent (Biotecx Inc., Houston, TX). First strand cDNA was synthesized using avian myoblastosis virus reverse transcriptase (Promega, Madison, WI).

Real-time PCR

Real-time PCR was performed in the iCycler iQ™ system (Bio-Rad, Hercules, CA) for 35 cycles of 25 sec at 95° C followed by 45 sec at 60° C. PCR primers used were as follows:

GAPDH	F: 5′-GAATCTACTGGCGTCTTCACC-3′ R: 5′-GTCATGAGCCCTTCCACGATGC-3′
ICP 27	F: 5′-TTCTCCAGTGCTACCTGAACC-3′ R: 5′-TCAACTCGCAGACACGACTCG-3′
TK	F: 5′-ATGGCTTCGTACCCCTGCCAT-3′ R: 5′-GGTATCGCGCGGCCGGGTA-3′
VP 16	F: 5′-GGACTGTATTCCAGCTTCAC-3′ R: 5′-CGTCCTCGCCGTCTAAGTG-3′
PKR	F: 5′-GGAAAATCCCGAACAAGGAG-3′ R: 5′-CCCAAAGCAAAGATGTCCAC-3′
OAS1a	F: 5′-ATTACCTCCTTCCCGACACC-3′ R: 5′-CAAACTCCACCTCCTGATGC-3′

A PCR supermix from Bio-Rad (iQ™ SYBR Green supermix containing Taq DNA polymerase, $MgCl_2$, dNTPs, SYBR Green I, and flourescein) was used. Primers were added to the reaction mix at a final concentration of 100 nM. A melting curve showed only one peak with no existing primer-dimer product. To confirm the absence of primer dimers, 1 % agarose gel analysis verified the amplification of one product of the predicted size with no primer-dimer bands. All reactions were run for 35 cycles at 95° C (30 sec), followed by 60° C (50 sec). Targeted gene expression data was analyzed quantitatively using the comparative C_T method. For each gene the threshold at which product was detected (10 standard deviations above the background signal) was compared to the endogenous (GAPDH) control. Prior to commencing studies, the comparative C_T method was validated by ensuring that the efficiencies of both the target gene and GAPDH primers were approximately equal. Results were calculated as C_T, i.e. the difference between the gene and GAPDH mean thresholds and are expressed in relative values calculated as previously described (29).

Statistics

One-way analysis of variance (ANOVA) and Tukey's t-test were used to determine significant (p<0.05) differences among the Ad:IFN-β–, Ad:Null-, and non-treated groups relative to IFN-β production, viral load, and cellular gene expression, using the Statistica program (Stat soft, Tulsa, OK). For the cumulative survival experiment, the non-parametric Mann-Whitney rank order test was used to determine significance.

Results

Topical application of the Ad:GFP to the cornea results in GFP expression in the cornea and the trigeminal ganglia

To assess the efficiency of the adenoviral vector to transduce mouse cornea, Ad:GFP was applied topically to scarified corneas. Corneas of the anesthetized mice were examined using a fluorescent dissecting microscope. Green fluorescence was seen as early as day 2 p.t. (Fig. 1A) and persisted up to 15 days p.t. No fluorescence was detected by day 18 p.t. Based on flat mount data (Fig. 1C), the transduced cells expressing GFP were located in the epithelial layer of the cornea (i.e. adjacent cells in high densities compared to stromal cells that are more dispersed and much fewer in number). In an attempt to increase the duration of the transgene expression, a different route for transduction was attempted. The Ad:GFP construct was injected into the corneal stroma of mice and GFP expression was evaluated as described above. The transduction, however, was localized to the site of the injection (Fig. 1B). The signal persisted for 19 days but disappeared by 22 days p.t. Therefore, in terms of duration of transgene expression, intrastromal administration possessed a marginal benefit over topical administration.

Since the cornea is highly innervated, it was possible that the viral vector may traffic to the sensory ganglion innervating the anterior segment of the eye. To this end, Ad:GFP was applied topically to scarified corneas and the mice were euthanized 3 days p.t. Using the fluorescent dissecting microscope, no green fluorescence was observed when the whole TG organ was examined. However, when the TGs were dissociated and cultured, GFP expression was present in a very small number of cells (0.4 +/− 0.2%) in the primary TG

culture. To characterize the nature of those GFP-expressing cells, dissociated TG cultures were co-stained for GFP and NSE. Cells that were positive for GFP were also positive for NSE (Fig. 1D, E, F). No cells expressing GFP were identified that did not also co-express NSE. These results indicate that the transgene is expressed proximal to the initial site of application (i.e., corneal epithelium) as well as sites distal including neurons located in the TG.

Ad:IFN-β augments survival and antagonizes viral replication in HSV-1 infected mice

Since the adenoviral vector was found to efficiently transduce the mouse cornea, an Ad:IFN-β vector was tested for its effectiveness in preventing viral-mediated pathogenesis following ocular infection. Initially, corneal buttons transduced *in vivo* with the Ad:IFN-β vector were assessed for detection of biologically active IFN. The results found transduced corneal explants produced 3.4 +/− 1.0 U of IFN-β per corneal button. In contrast, corneal buttons transduced with the Ad:Null secreted no detectable biologically active IFN. Consistent with the expression of biologically active IFN-β in the cornea, Ad:IFN-β transduced mice showed enhanced survival compared to vehicle (PBS) or Ad:Null transduced mice (Fig. 2). The protective effect was observed whether the transduction preceded the infection by 2 (Fig. 2A) or 4 (Fig. 2B) days. Likewise, a protective effect was observed if transduction occurred simultaneously with infection (Fig 3). However, the benefit for Ad:IFN-β was reduced if the transduction was delayed 24 hr after infection (Fig. 3). In mice transduced 7 prior to infection there was marginal protection. Specifically, mice transduced with Ad:IFN-β succumbed to HSV-1 infection at a slower rate as compared to the control groups, but the final outcome was not different between the groups of transduced mice (data not shown). Coincident with enhanced survival, Ad:IFN-β transduced mice showed a dramatic reduction in viral titer (Fig. 4) and viral gene expression (Fig. 5) in both the eyes and TG during the acute period of infection. Relative to viral gene expression, mice treated with Ad:IFN-β expressed significantly lower immediate early (ICP27) and early (TK) transcript levels in both the eyes and the TGs at days 3 and 6 p.i (Fig. 5). The HSV-1 late gene VP16 was expressed at a lower level in the corneas and TGs of Ad:IFN-β transduced mice only at day 6 but not day 3 p.i..

Mice treated with Ad:IFN-β express lower IFN-γ levels and reduced CD8+ T lymphocyte and NK cell infiltration in the TG

Acute HSV-1 infection of the cornea results in the retrograde transport of the virus from the anterior segment of the eye to the sensory ganglia initiating replication at this site as well. As a result of viral antigen expression within the TG, an intense inflammatory response is noted with T lymphocyte, macrophage, and NK cell infiltration and the expression of cytokines including IFN-γ (36–38). Since there is evidence to support polarization of the immune response by type I IFN (19,39) and the transgene is expressed in the TG following *in situ* transduction of the eye (Fig. 1D), it was hypothesized that transduction of mice with the Ad:IFN-β vector would modify the local (i.e., TG) immune response following HSV-1 infection. To investigate the effects of Ad:IFN-β transduction on the nature of the immune reaction in the TG, mice were ocularly transduced with Ad:IFN-β or Ad:Null and infected with HSV-1 two days later. Seven days p.i., TGs were extracted and IFN-γ level as well as the composition of inflammatory cells infiltrating the TG were determined. IFN-γ transcript

and protein levels were significantly reduced in the TGs from Ad:IFN-β transduced mice compared to the Ad:Null transduced group (Table I). The transduction with the adenoviral vector alone had no effect on the level of IFN-γ expressed in the TG. Associated with changes in the IFN-γ levels were changes in the infiltrating lymphocyte population. Specifically, Ad:IFN-β transduced mice showed a significant reduction in the percentage of CD8^{+} T lymphocytes and NK cells infiltrating the TG in comparison to Ad:Null transduced mice 7 days p.i. (Table I, Fig. 6). However, there was no detectable CD4^{+} T lymphocyte infiltration in any of the groups. Consequently, it would appear that changes in the IFN-γ levels simply reflect changes in the infiltrating effector cells in the Ad:IFN-β transduced mice. Moreover, the results suggest that the composition of the inflammatory reaction in the TG correlates with the antigenic load rather than a direct modification by IFN-β.

Ad:IFN-β specifically up-regulates OAS expression in the cornea and TG

Two prominent anti-viral pathways responsive to type I IFN and previously shown to be involved in suppression of HSV-1 replication include OAS and PKR (3, 8–10). Since it was found that Ad:IFN-β transduction of the cornea suppressed viral replication in the cornea and TG, we hypothesized that the suppression was due to the activation of the OAS and/or PKR pathway. Therefore, mice transduced in the cornea with Ad:IFN-β were assessed for OAS1a and PKR transcript levels using real-time PCR. Transcript levels of OAS1a were higher in both the cornea and the TG in mice transduced with the Ad:IFN-β vector compared to mice transduced with the Ad:Null vector or PBS (Table II). Surprisingly, no significant change in PKR transcript expression was found in either the cornea or the TG.

The absence of a functional OAS pathway transiently diminishes the anti-viral effect of the Ad:IFN-β vector in the cornea but not TG

To delineate the potential relevance of the OAS pathway in inhibiting HSV-1 replication following transduction of mice with the Ad:IFN-β vector, mice deficient in RNase L enzyme (RL–/–) and the wild type counterparts (RL+/+) were employed. Consistent with previous results using outbred ICR mice, RL+/+ mice transduced with the Ad:IFN-β vector prior to HSV-1 challenge had significantly reduced viral titers in the corneas and the TGs 3 or 6 days p.i. (Fig. 7A & B). In the absence of a functional OAS pathway, Ad:IFN-β transduction yielded lower viral titers and viral gene expression in the TGs of recipient animals similar to RL+/+ controls (Fig. 7B). In contrast, the anti-viral environment established following Ad:IFN-β transduction was transiently lost in the cornea 3 days p.i. (Fig. 7A). However, by day 6 p.i., the absence of a functional OAS pathway did not significantly impact on the anti-viral efficacy of the Ad:IFN-β vector in the RL–/– mice. It should also be noted that the absence of a functional OAS pathway did not significantly increase the viral load measured in infected tissue comparing the wild type to RL–/– mice. We interpret these results to suggest that the constitutive OAS pathway does not have a central role in antagonizing HSV-1 replication in either the eye or TG in the absence of exogenous IFN.

The anti-viral action of Ad:IFN-β is adversely affected in mice deficient in PKR protein

Although there was no indication of an increase in PKR expression upon transduction of mice with the Ad:IFN-β vector, the constitutive level of PKR may still have a significant impact on the anti-viral nature of the Ad:IFN-β vector in the mice. This notion is supported

by the observation showing an attenuated HSV-1 mutant that fails to thrive in wild type mice replicates to similar efficiency as parental virus in PKR knockout mice (10). To address the role of PKR in the IFN-induced anti-viral action, mice deficient in PKR (PKR−/ −) were used to evaluate the efficacy of the Ad:IFN-β vector in measuring viral replication and lytic gene expression in the cornea and TG following HSV-1 infection. PKR−/− mice transduced with the control vector Ad:Null were more susceptible to HSV-1 infection as compared to the wild type group. Specifically, elevated viral titers and viral gene levels were detected in the PKR knockout mice indicating a role for PKR in the absence of exogenous stimuli in antagonizing ocular HSV-1 infection (Fig. 7C & D). Similar to the results using the RL−/− mice, the Ad:IFN-β vector was efficient in inhibiting viral replication in PKR−/− mice as well as in the wild type group during acute infection surveyed 3 and 6 days p.i. (Fig. 7C & D). However, the magnitude of reduction observed in the Ad:IFN-β transduced PKR−/ − mice was significantly less compared to that found in the wild type controls and that effect was most evident at the 6 day p.i. time point. Specifically, in wild type mice, there was a > 2 log reduction in the viral titer recovered from the cornea and TG compared to approximately a 1 log reduction in viral titer in the PKR knockout mice. We interpret these results to suggest that while PKR is not absolutely required for resistance to ocular HSV-1 following transduction with the Ad:IFN-β vector, it does have a profound effect on the efficiency of clearance of virus demonstrated by infectious virions recovered from infected tissue of the Ad:IFN-β transduced mice compared to the transduced wild type controls.

Discussion

Gene transfer to the cornea is an appealing approach to tackle many diseases that affect this organ, including HSV-1 infection. The outermost layer of the cornea (the epithelium) has been a challenging tissue for gene therapy (40, 41). In this study, the successful transfer and expression of murine IFN-β to the corneal epithelium using an adenoviral vector applied directly onto scarified corneas was demonstrated. The expression was diffuse and mostly located along scarification lines. However, the duration of transgene expression was limited to 14 days. In addition, the topical application of the adenoviral vector was associated with transgene expression in the TG demonstrating a neurotropic attribute for this vector. Consistent with the present results, previous studies have reported the translocation of adenoviral vectors to neuronal bodies upon application of the virus in peripheral tissue (42, 43). The ability of the adenoviral vector to utilize retrograde transport to sensory ganglia has also been demonstrated using other viruses including alphaviruses (44) and rhabdoviruses (45). In addition, HSV-1 based vectors also transduce neurons and are delivered by rapid retrograde axonal transport via neurites to the soma providing a means of targeting cells that are difficult to reach (46, 47).

The use of an adenoviral vector expressing IFN-β was successful in protecting mice against HSV-1 induced mortality. The protection was associated with a reduction in viral titer and viral gene expression both in the cornea and the TG at 3 and 6 days p.i. These results demonstrate the feasibility of using a viral-based gene therapy approach to control HSV-1 infection. The limited transgene expression using adenoviral vectors is expected to be a major concern. The corneal epithelium is a renewable tissue composed of a proliferating basal layer, which is believed to contain keratinocyte stem cells, and a suprabasal layer

above the dividing layer composed of non-dividing keratinocytes undergoing progressive differentiation. Keratinocyte stem cells exist as slowly cycling cells in the basal layers of the epidermis *in vivo* (48) and are the progenitor cells for the epithelium (49). Achieving persistent and high-level gene expression in a significant percentage of target cells is important for establishing a successful clinical application for gene transfer. The limited duration of transgene expression in this study could be due to the transduction of the outermost layer, which naturally exfoliates losing the transgene with it. This process was evident in the present study by demonstrating the loss of GFP expression by scarification of transduced cornea of euthanized mice (day 4–5 post transduction, data not shown). It could also be due to the nature of adenoviral vectors, which deliver the transgene as part of an extra chromosomal episome (50). For gene therapy of the corneal epithelium, a renewable tissue undergoing constant turnover and for achieving long-term expression in a significant percentage of keratinocytes, gene targeting to stem cells will be required. This approach seems very plausible using lentiviruses as a potential delivery system for gene transfer (51). Several labs have demonstrated long-term expression associated with lentivirus transduction of epithelial stem cells (52–54). Alternatively, because of the highly innervated nature of the cornea, the possible use of viral vectors to deliver genes directly to the neurons of the sensory ganglion as demonstrated in the present study may have significant consequences to viral reactivation, for example, with HSV-1.

Ocular HSV-1 infection results in the infiltration of CD8^{+} T lymphocytes and NK cells into the TG. No CD4^{+} T cells were noted in the TG of infected mice. Transduction with the Ad:IFN-β vector reduced CD8^{+} T and NK cell infiltration with a significant reduction in IFN-γ levels. The reduction in the inflammatory reaction was most likely due to the lack of antigenic stimulus in Ad:IFN-β treated mice and not by direct IFN action on the immune system. However, IFN-β has been reported to reduce perivascular infiltration in a rodent model of acute EAE by suppressing the expression of the adhesion molecules ICAM-1 and VCAM-1 on brain capillaries (55). Consequently, a reduction in lymphocyte infiltration into the infected ganglion in the Ad:IFN-β transduced mice may have resulted from such an outcome. Collectively, these results reaffirm previous observations showing that MHC class II-restricted CD4^{+} T cells are primarily responsible for clearing HSV from the cornea, whereas MHC class I-restricted CD8^{+} cytotoxic T lymphocytes are the predominant effectors that control HSV replication in the nervous system (56).

RL−/− mice were not found to be more susceptible to ocular HSV-1 infection compared to the wild type control group. However, exogenous expression of type I IFN following transduction of RL−/− mice with the Ad:IFN-β vector resulted in a transient attenuation of the anti-viral effect restricted to the cornea in these mice. Specifically, the impact of Ad:IFN-β on viral titers expression in the corneas of RL−/− mice was attenuated at day 3 p.i.. The OAS pathway is a key component of the innate immune system against several viruses such as vaccinia virus, reovirus, and encephalomyocarditis (EMCV) (57). However, the phenotype resulting from lacking a functional OAS pathway is more evident when an exogenous source of IFN is administered either *in vitro* or *in vivo* (3, 34, 58). In fact, the level of activation of the OAS pathway seems to be directly related to the concentration of IFN at the site of infection (3). The tissue specific nature of IFN-responsive, anti-viral

pathways is not unique to OAS as a previous study showed tissue tropism exists for the PKR pathway as well (59).

The current results demonstrate a role for PKR in the resistance against HSV-1 infection compared to that of OAS. However, similar to the results using the RL−/− mice, the phenotype associated with a lack of PKR becomes more evident in the presence of exogenous IFN-β. It is important to note though, that IFN-β retained some activity even in the absence of PKR. Additional studies using influenza and vaccinia viruses as well as VSV have noted either a critical or minimal requirement for PKR in suppressing viral replication or viral-mediated pathogenesis *in vivo* (59, 60). Consequently, the dichotomy depicting the central role of PKR in controlling viral infection *in vitro* (3, 10, 61, 62) and in some cases, a more modest role *in vivo* (60, present findings) strongly implicate additional pathways are involved in antagonizing viral replication including HSV-1 (58).

In conclusion, this study demonstrates the efficacy of using adenoviral vectors to transduce mouse corneas with the murine IFN-β transgene. To the best of our knowledge, this is the first study to investigate the involvement of both the PKR and OAS pathways following the *in situ* administration of an exogenous source of type I IFN. We have documented the transient involvement of OAS in the cornea in the presence of IFN-β. A more dramatic need for PKR was observed in the presence of exogenous IFN-β in both the cornea and TG with a log increase in the viral yield recovered in these tissues in the PKR knockout mice compared to the wild type controls. In addition to the well-defined anti-viral action of PKR, this pathway has also been found to promote apoptosis (63) and regulate CD8^{+} T cell function (64) requiring further exploration into the action of these components and type I IFN relative to ocular HSV-1 infection. Finally, the present findings demonstrate proof of principal regarding the capacity to deliver an anti-viral transgene to the cornea and associated ganglion and the establishment of an environment resistant to viral replication. The ultimate challenge will be to identify a delivery system that provides long-term and site-specific expression of the transgene in the cornea and/or sensory ganglion preventing reactivation of latent HSV-1 and the disease associated with episodic reactivation, herpetic keratitis.

Acknowledgments

References

1. Kerr IM, Brown RE. pppA2′p5′A2′p5′A: an inhibitor of protein synthesis synthesized with an enzyme fraction from interferon-treated cells. Proc Natl Acad Sci U S A. 1978; 75:256. [PubMed: 272640]

2. Silverman, RH. 2–5 A-dependent RNase L: a regulated endoribonuclease in the interferon system. In: Riordan, GDAJF., editor. Ribonucleases: Structure and Function. Academic Press; New York: 1997. p. 515

3. Al-Khatib K, Williams BR, Silverman R, Halford WP, Carr DJ. The murine double-stranded RNA-dependent protein kinase PKR and murine 2′, 5′-oligoadenylate synthetase-dependent RNase L are required for IFN-b-mediated resistance against herpes simplex virus type 1 in primary trigeminal ganglion culture. Virology. 2003; 313:126. [PubMed: 12951027]

4. Meurs E, Chong K, Galabru J, Thomas NS, Kerr IM, Williams BR, Hovanessian AG. Molecular cloning and characterization of the human double-stranded RNA- activated protein kinase induced by interferon. Cell. 1990; 62:379. [PubMed: 1695551]

5. Katze MG, Wambach M, Wong ML, Garfinkel M, Meurs E, Chong K, Williams BR, Hovanessian AG, Barber GN. Functional expression and RNA binding analysis of the interferon- induced, double-stranded RNA-activated, 68,000-Mr protein kinase in a cell-free system. Mol Cell Biol. 1991; 11:5497. [PubMed: 1717830]

6. Meurs EF, Watanabe Y, Kadereit S, Barber GN, Katze MG, Chong K, Williams BR, Hovanessian AG. Constitutive expression of human double-stranded RNA-activated p68 kinase in murine cells mediates phosphorylation of eukaryotic initiation factor 2 and partial resistance to encephalomyocarditis virus growth. J Virol. 1992; 66:5804.

7. Williams BR. Signal integration via PKR. Sci STKE. 2001; 2001:RE2. [PubMed: 11752661]

8. Khabar KSA, Dhalla M, Siddiqui Y, Zhou A, Al-Ahdal MN, Der SD, Silverman RH, Williams BRG. Effect of deficiency of the double-stranded RNA-dependent protein kinase, PKR, on antiviral resistance in the presence or absence of ribonuclease L: HSV-1 replication is particularly sensitive to deficiency of the major IFN-mediated enzymes. J Interferon Cytokine Res. 2000; 20:653. [PubMed: 10926208]

9. Al-Khatib K, Williams BR, Silverman RH, Halford WP, Carr DJ. Absence of PKR attenuates the anti-HSV-1 activity of an adenoviral vector expressing murine IFN-beta. J Interferon Cytokine Res. 2002; 22:861. [PubMed: 12396725]

10. Leib DA, Machalek MA, Williams BRG, Silverman RH, Virgin HW. Specific phenotypic restoration of an attenuated virus by knockout of a host resistance gene. Proc Natl Acad Sci USA. 2000; 97:6097–6101. [PubMed: 10801979]

11. Adler H, Beland JL, Del-Pan NC, Kobzik L, Sobel RA, Rimm IJ. In the absence of T cells, natural killer cells protect from mortality due to HSV-1 encephalititis. J Neuroimmunol. 1999; 93:208. [PubMed: 10378885]

12. Biron CA, Nguyen K, Pien GC, Cousens LP, Salazar-Mather TP. Natural killer cells in antiviral defense: function and regulation by innate cytokines. Annu Rev Immunol. 1999; 17:189. [PubMed: 10358757]

13. Montoya M, Schiavoni G, Mattei F, Gresser I, Belardelli F, Borrow P, Tough DF. Type I interferons produced by dendritic cells promote their phenotypic and functional activation. Blood. 2002; 99:3263. [PubMed: 11964292]

14. Mattei F, Schiavoni G, Belardelli F, Tough DF. IL-15 is expressed by dendritic cells in response to type I IFN, double-stranded RNA, or lipopolysaccharide and promotes dendritic cell activation. J Immunol. 1999; 167:1179. [PubMed: 11466332]

15. Fawaz LM, Sharif-Askari E, Menezes J. Up-regulation of NK cytotoxic activity via IL-15 induction by different viruses: A comparative study. J Immunol. 1999; 163:4473. [PubMed: 10510389]

16. Ahmad A, Sharif-Askari E, Fawaz L, Menezes J. Innate immune response of the human host to exposure with herpes simplex virus type 1: In vitro control of the virus infection by enhanced natural killer activity via interleukin-15 induction. J Virol. 2000; 74:7196. [PubMed: 10906173]

17. Parlato S, Santini SM, Lapenta C, Di Pucchio T, Logozzi M, Spada M, Giammarioli AM, Malorni W, Fais S, Belardelli F. Expression of CCR-7, MIP-3beta, and Th-1 chemokines in type I IFN-induced monocyte-derived dendritic cells: importance for rapid acquisition of potent migratory and functional activities. Blood. 2001; 98:3022. [PubMed: 11698286]

18. Carr DJJ, Chodosh J, Ash J, Lane TE. Effect of anti-CXCL10 monoclonal antibody on herpes simplex virus type 1 keratitis and retinal function. J Virol. 2003; 77:10037. [PubMed: 12941914]

19. Biron CA. Interferons alpha and beta as immune regulators--a new look. immunity. 2001; 14:661. [PubMed: 11420036]

20. Hendricks RL, Weber PC, Taylor JL, Koumbis A, Tumpey TM, Glorioso JC. Endogenously produced interferon α protects mice from herpes simplex virus type 1 corneal disease. J Gen Virol. 1991; 72:1601. [PubMed: 1649898]

21. Brandt CR, Salkowski CA. Activation of NK cells in mice following corneal infection with herpes simplex virus type-1. Invest Ophthalmol Res Vis Sci. 1992; 33:113.

22. Tumpey TM, Chen SH, Oakes JE, Lausch RN. Neutrophil-mediated suppression of virus replication after herpes simplex virus type 1 infection of the murine cornea. J Virol. 1996; 70:898. [PubMed: 8551629]

23. Cheng H, Tumpey TM, Staats HF, van Rooijen N, Oakes JE, Lausch RN. Invest Ophthalmol Vis Sci. 2000; 41:1402. [PubMed: 10798656]

24. Niemialtowski MG, Rouse BT. Phenotypic and functional studies on ocular T cells during herpetic infections of the eye. J Immunol. 1992; 148:1864. [PubMed: 1347309]

25. Carr DJJ, Noisakran S. The antiviral efficacy of the murine alpha-1 interferon transgene against ocular herpes simplex virus type 1 requires the presence of CD4$^+$, α/β T-cell receptor-positive T lymphocytes with the capacity to produced gamma interferon. J Virol. 2002; 76:9398. [PubMed: 12186922]

26. Minami M, Kita M, Yan XQ, Yamamoto T, Iida T, Sekikawa K, Iwakura Y, Imanishi J. J Interferon Cytokine Res. 2002; 22:671. [PubMed: 12162877]

27. Balish MJ, Abrams ME, Pumfery AM, Brandt CR. Enhanced inhibition of herpes simplex virus type 1 growth in human corneal fibroblasts by combinations of interferon-alpha and -gamma. J Infect Dis. 1992; 166:1401. [PubMed: 1331251]

28. Sainz B, Halford WP. Alpha/beta interferon and gamma interferon synergize to inhibit the replication of herpes simplex virus type 1. J Virol. 2002; 76:11451.

29. Harle P, Cull V, Agbaga MP, Silverman R, Williams BR, James C, Carr DJJ. Differential effect of murine alpha/beta interferon transgenes on antagonization of herpes simplex virus type 1 replication. J Virol. 2002; 76:6558. [PubMed: 12050368]

30. Tuohy VK, Yu M, Yin L, Mathisen PM, Johnson JM, Kawczak JA. Modulation of the IL-10/IL-12 cytokine circuit by interferon-β inhibits the development of epitope spreading and disease progression in murine autoimmune encephalomyelitis. J Neuroimmunol. 2000; 111:55. [PubMed: 11063821]

31. McRae BL, Beilfuss BA, van Seventer GA. IFN-β differentially regulates CD40-induced cytokine secretion by human dendritic cells. J Immunol. 2000; 164:23. [PubMed: 10604988]

32. Hendricks RL, Tumpey TM, Finnegan A. IFN-γ and IL-2 are protective in the skin but pathologic in the cornea of HSV-1-infected mice. J Immunol. 1992; 149:3023. [PubMed: 1401927]

33. Tang Q, Hendricks RL. Interferon γ regulates platelet endothelial cell adhesion molecule 1 expression and neutrophil infiltration into herpes simplex virus-infected mouse cornea. J Exp Med. 1996; 184:1435. [PubMed: 8879215]

34. Zhou A, Paranjape J, Brown TL, Nie H, Naik S, Dong B, Chang A, Trapp B, Fairchild R, Colmenares C, Silverman RH. Interferon action and apoptosis are defective in mice devoid of 2′, 5′-oligoadenylate-dependent RNase L. EMBO J. 1997; 16:6355. [PubMed: 9351818]

35. Yang YL, Reis LF, Pavlovic J, Aguzzi A, Schafer R, Kumar A, Williams BR, Aguet M, Weissmann C. Deficient signaling in mice devoid of double-stranded RNA-dependent protein kinase. Embo J. 1995; 14:6095. [PubMed: 8557029]

36. Shimeld C, Whiteland JL, Nicholls SM, Grinfeld E, Easty DL, Gao H, Hill TJ. Immune cell infiltration and persistence in the mouse trigeminal ganglion after infection of the cornea with herpes simplex virus type 1. J Neuroimmunol. 1995; 61:7. [PubMed: 7560014]

37. Cantin E, Hinton DR, Chen J, Openshaw H. Gamma interferon expression during acute and latent nervous system infection by herpes simplex virus type 1. J Virol. 1995; 69:4898. [PubMed: 7609058]

38. Liu T, Tang Q, Hendricks RL. Inflammatory infiltration of the trigeminal ganglion after herpes simplex virus type 1 corneal infection. J Virol. 1996; 70:264. [PubMed: 8523535]

39. Brinkmann V, Geiger T, Alkan S, Heusser CH. Interferon alpha increases the frequency of interferon gamma-producing human CD4+ T cells. J Exp Med. 1993; 178:1655. [PubMed: 8228812]

40. Tanelian DL, Barry MA, Johnston SA, Le T, Smith G. Controlled gene gun delivery and expression of DNA within the cornea. Biotech. 1997; 23:484.

41. Tsubota K, Inoue H, Ando K, Ono M, Yoshino K, Saito I. Adenovirus-mediated gene transfer to the ocular surface epithelium. Exp Eye Res. 1998; 67:531. [PubMed: 9878215]

42. Soudais C, Laplace-Builhe C, Kissa K, Kremer EJ. Preferential transduction of neurons by canine adenovirus vectors and their efficient retrograde transport in vivo. Faseb J. 2001; 15:2283. [PubMed: 11511531]

43. Finiels F, Gimenez Y, Ribotta M, Barkats M, Samolyk ML, Robert JJ, Privat A, Revah F, Mallet J. Specific and efficient gene transfer strategy offers new potentialities for the treatment of motor neurone diseases. Neuroreport. 1995; 7:373. [PubMed: 8742491]

44. Strauss JH, Strauss EG. The alphaviruses: gene expression, replication, and evolution. Microbiol Rev. 1994; 58:491. [PubMed: 7968923]

45. Tsiang H. Evidence for an intraaxonal transport of fixed and street rabies virus. Journal of Neuropathology & Experimental Neurology. 1979; 38:286. [PubMed: 86604]

46. Geller AI, Keyomarsi K, Bryan J, Pardee AB. An efficient deletion mutant packaging system for defective herpes simplex virus vectors: potential applications to human gene therapy and neuronal physiology. Proc Natl Acad Sci U S A. 1990; 87:8950. [PubMed: 2174168]

47. Palella TD, Hidaka Y, Silverman LJ, Levine M, Glorioso J, Kelley WN. Expression of human HPRT mRNA in brains of mice infected with a recombinant herpes simplex virus-1 vector. Gene. 1989; 81:137. [PubMed: 2551779]

48. Cotsarelis G, Cheng SZ, Dong G, Sun TT, Lavker RM. Existence of slow-cycling limbal epithelial basal cells that can be preferentially stimulated to proliferate: implications on epithelial stem cells. Cell. 1989; 57:201. [PubMed: 2702690]

49. Lavker RM, Sun TT. Epidermal stem cells: properties, markers, and location. Proc Natl Acad Sci U S A. 2000; 97:13473. [PubMed: 11087834]

50. St George JA. Gene therapy progress and prospects: adenoviral vectors. Gene Ther. 2003; 10:1135. [PubMed: 12833122]

51. Jakobsson J, Ericson C, Rosenqvist N, Lundberg C. Lentiviral vectors. Int Rev Neurobiol. 2003; 55:111. [PubMed: 12968533]

52. Kuhn U, Terunuma A, Pfutzner W, Foster RA, Vogel JC. In vivo assessment of gene delivery to keratinocytes by lentiviral vectors. J Vir. 2002; 76:1496.

53. Ghazizadeh S, Doumeng C, Taichman LB. Durable and stratum-specific gene expression in epidermis. Gene Ther. 2002; 9:1278. [PubMed: 12224010]

54. Wang X, Appukuttan B, Ott S, Patel R, Irvine J, Song J, Park JH, Smith R, Stout JT. Efficient and sustained transgene expression in human corneal cells mediated by a lentiviral vector. Gene Ther. 2000; 7:196. [PubMed: 10694795]

55. Floris S, Ruuls SR, Wierinckx A, van der Pol SMA, Dopp E, van der Meide PH, Dijkstra CD, De Vries HE. Interferon-β directly influences monocyte infiltration into the central nervous system. J Neuroimmunol. 2002; 127:69. [PubMed: 12044977]

56. Nash AA, Jayasuriya A, Phelan J, Cobbold SP, Waldmann H, Prospero T. Different roles for L3T4+ and Lyt 2+ T cell subsets in the control of an acute herpes simplex virus infection of the skin and nervous system. J Gen Virol. 1987; 68:825. [PubMed: 2950204]

57. Zhou A, Paranjape JM, Hassel BA, Nie H, Shah S, Galinski B, Silverman RH. Impact of RNase L overexpression on viral and cellular growth and death. J Interferon Cytokine Res. 1998; 18:953. [PubMed: 9858317]

58. Zhou A, Paranjape JM, Der SD, Williams BR, Silverman RH. Interferon action in triply deficient mice reveals the existence of alternative antiviral pathways. Virology. 1999; 258:435. [PubMed: 10366581]

59. Stojdl DF, Abraham N, Knowles S, Marius R, Brasey A, Lichty BD, Brown EG, Sonenberg N, Bell JC. The murine double-stranded RNA-dependent protein kinase PKR is required for resistance to vesicular stomatitis virus. J Virol. 2000; 74:9580. [PubMed: 11000229]

60. Abraham N, Stojdl DF, Duncan PI, Methot N, Ishii T, Dube M, Vanderhyden BC, Atkins HL, Gray DA, McBurney MW, Koromilas AE, Brown EG, Sonenberg N, Bell JC. Characterization of transgenic mice with targeted disruption of catalytic domain of the double-stranded RNA-dependent protein kinase, PKR. J Biol Chem. 1999; 274:5953. [PubMed: 10026221]

61. Der SD, Lau AS. Involvement of the double-stranded-RNA-dependent kinase PKR in interferon expression and interferon-mediated antiviral activity. Proc Natl Acad Sci U S A. 1995; 92:8841. [PubMed: 7568028]

62. Lee SB, Esteban M. The interferon-induced double-stranded RNA- activated human p68 protein kinase inhibits the replication of vaccinia virus. Virology. 1993; 193:1037. [PubMed: 8096351]

63. Clemens MJ. Interferons and apoptosis. J Interferon Cytokine Res. 2003; 23:277. [PubMed: 12859854]

64. Kadereit S, Xu H, Engeman TM, Yang YL, Fairchild RL, Williams BRG. Negative regulation of CD8^{+} T cell function by the IFN-induced and double-stranded RNA-activated kinase PKR. J Immunol. 2000; 165:6896. [PubMed: 11120814]
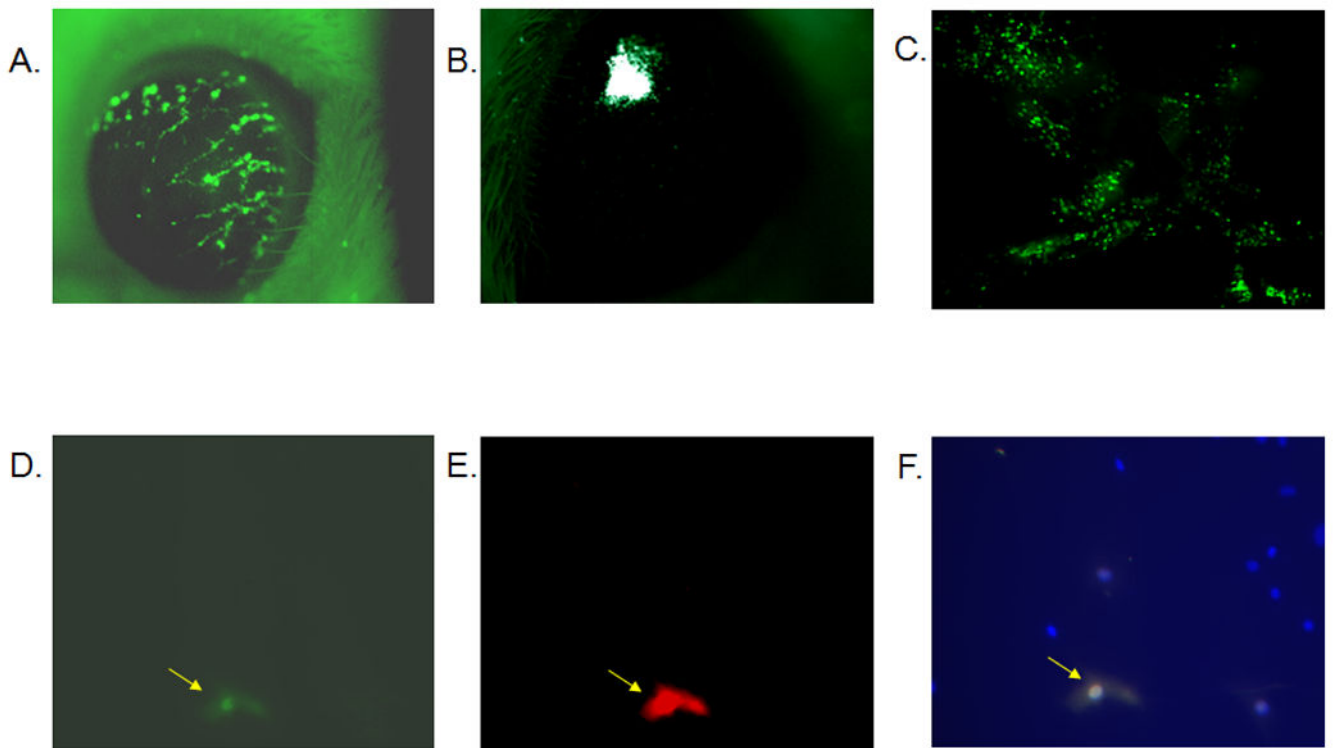
Figure 1. Ad:GFP application to the cornea results in GFP expression in the epithelial layer of the cornea, as well as GFP expression in the TG

ICR mice were anesthetized and the Ad:GFP vector (1×10^5 transducing units) was applied topically to scarified corneas. GFP expression was detected in the cornea at day 2 (A) as well as day 15 (data not shown) post transduction. Alternatively, Ad:GFP was injected into the corneal stroma resulting in localized expression detected at day 2 (B) as well as day 19 (data not shown) post transduction. (C) Flat mount of a cornea that was transduced 2 days before by direct application of Ad:GFP onto the scarified cornea. To detect any transgene expression in the TG, mice were transduced with the Ad:GFP vector by direct application of the vector onto scarified corneas. Three days later the TGs were extracted, collagenized and plated on laminin/collagen coated cover slips. Seven days later, cultures were fixed and stained for GFP (D) and neuron-specific enolase (E), and counterstained with DAPI. The combined image is shown in panel F.
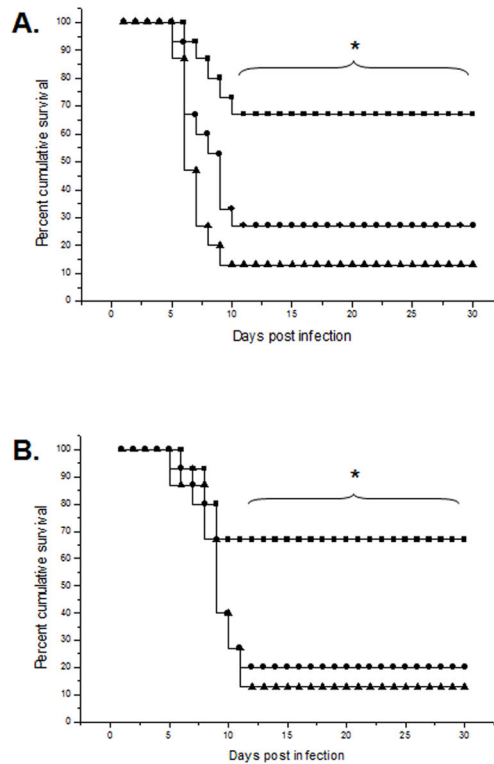
Figure 2. The Ad:IFN-β construct enhances the cumulative survival of mice ocularly infected with HSV-1

The corneas of ICR mice were scarified and transduced with either Ad:IFN-β or Ad:Null vectors (1×10^6 transducing units/eye) 2 (A) or 4 days (B) prior to infection with 150 pfu/eye HSV-1 (McKrae strain). Mortality was recorded for each group of animals. The squares represent Ad:IFN-β transduced mice, the circles represent Ad:Null transduced mice, and the triangles represent PBS-treated mice. This figure is a summary of three experiments (n = 5 mice/group per experiment). *$p<0.5$ comparing PBS- or Ad:Null-treated groups to Ad:IFN-β treated group at each indicated time point as determined using Mann Whitney rank order test.
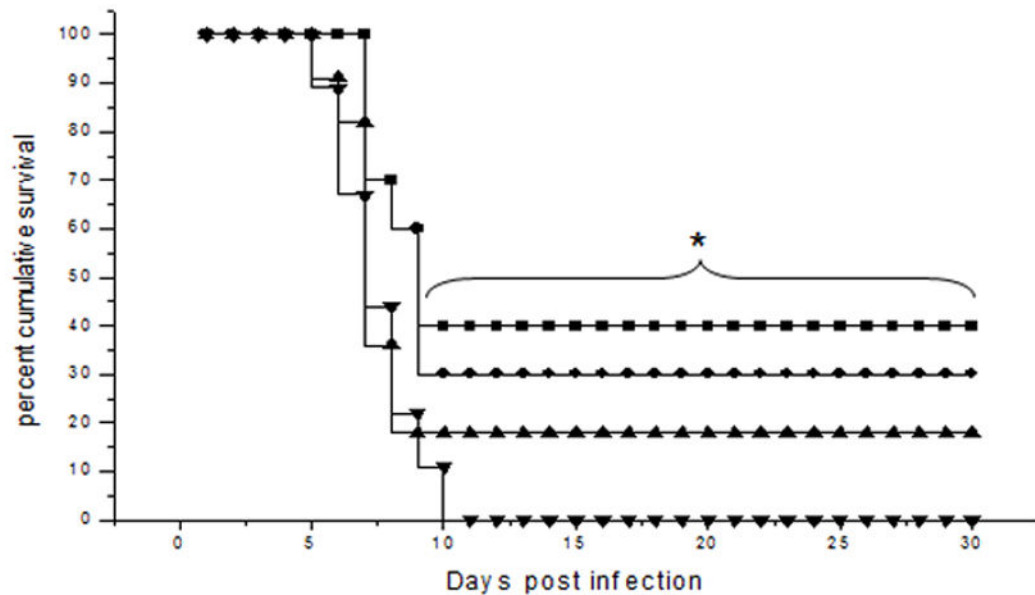
Figure 3. Ad:IFN-β transduction of the cornea at the time of ocular HSV-1 infection enhances survival of mice

The corneas of ICR mice were scarified and transduced with either Ad:IFN-β or Ad:Null vectors (1×10^6 transducing units/eye) at the time of or 24 hr prior to infection with 150 pfu/eye HSV-1 (McKrae strain). Mortality was recorded for each group of animals. The squares represent Ad:IFN-β transduction at the time of infection, the circles represent Ad:IFN-β transduction 24 hr prior to infection, the triangles represent the Ad:Null transduction at the time of infection, and the inverted triangles represent Ad:Null transduction 24 hr prior to infection. This figure is a summary of two experiments (n = 5–6 mice/group per experiment). *p<0.5 comparing Ad:Null to Ad:IFN-β groups transduced at the time of infection as determined using Mann Whitney rank order test.
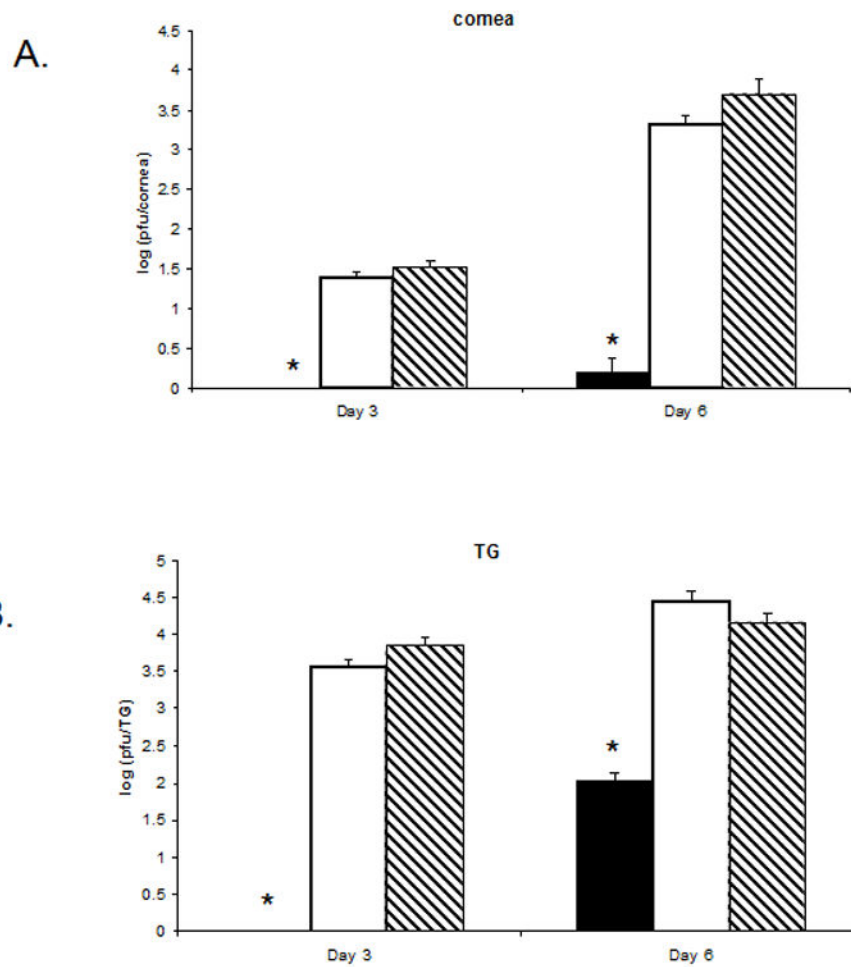
Figure 4. Ad:IFN-β transduction of the cornea antagonizes viral replication in both the eye and the TG of HSV-1 infected mice

Female ICR mice (n=4 per group/experiment) were transduced (1×10^6 transducing units/eye) with Ad:IFN-β (black column), Ad:Null (white column), or vehicle (PBS, dashed column). Two days later, the mice were infected with HSV-1 (150 pfu/eye). Mice were euthanized 3 or 6 days post infection, and the cornea (A) and the TG (B) were removed. The tissue was homogenized and the clarified homogenate ($10,000 \times g$, 1 min) was quantified for infectious virus by plaque assay. Results are a summary of two independent experiments. Bars represent the log of the mean +/− SEM. *$p<.05$ comparing the Ad:IFN-β to the Ad:Null- or vehicle-treated mice.
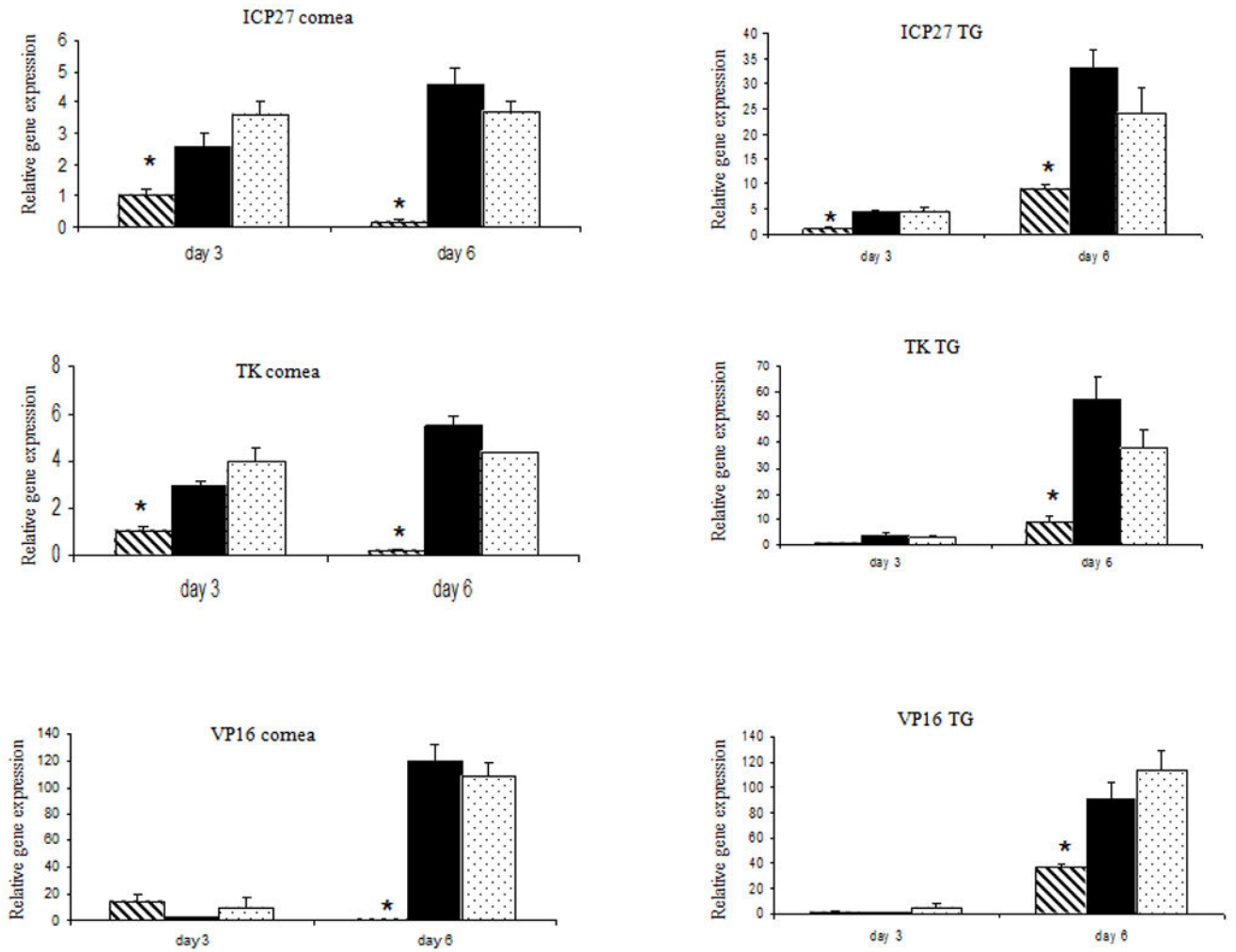
Figure 5. Mice transduced with Ad:IFN-β express show a reduction in the expression of the ICP27 and TK transcript levels in both the eye and the TG

Female ICR mice (n=4 per group/experiment) were transduced (1×10^6 transducing units) with Ad:IFN-β (dashed column), Ad:Null (black column), or vehicle (PBS, dotted column). Two days later, the mice were infected with HSV-1 (150 pfu/eye). Mice were euthanized 3 or 6 days post infection, and the cornea and the TG were removed. RNA was isolated and processed to cDNA. Real time PCR was performed to determine the relative gene expression in each sample of a representative panel of HSV-1 genes. Results are a summary of two independent experiments. Bars represent the mean +/− SEM. *p<.05 comparing the Ad:IFN-β to the Ad:Null- or vehicle-treated mice.
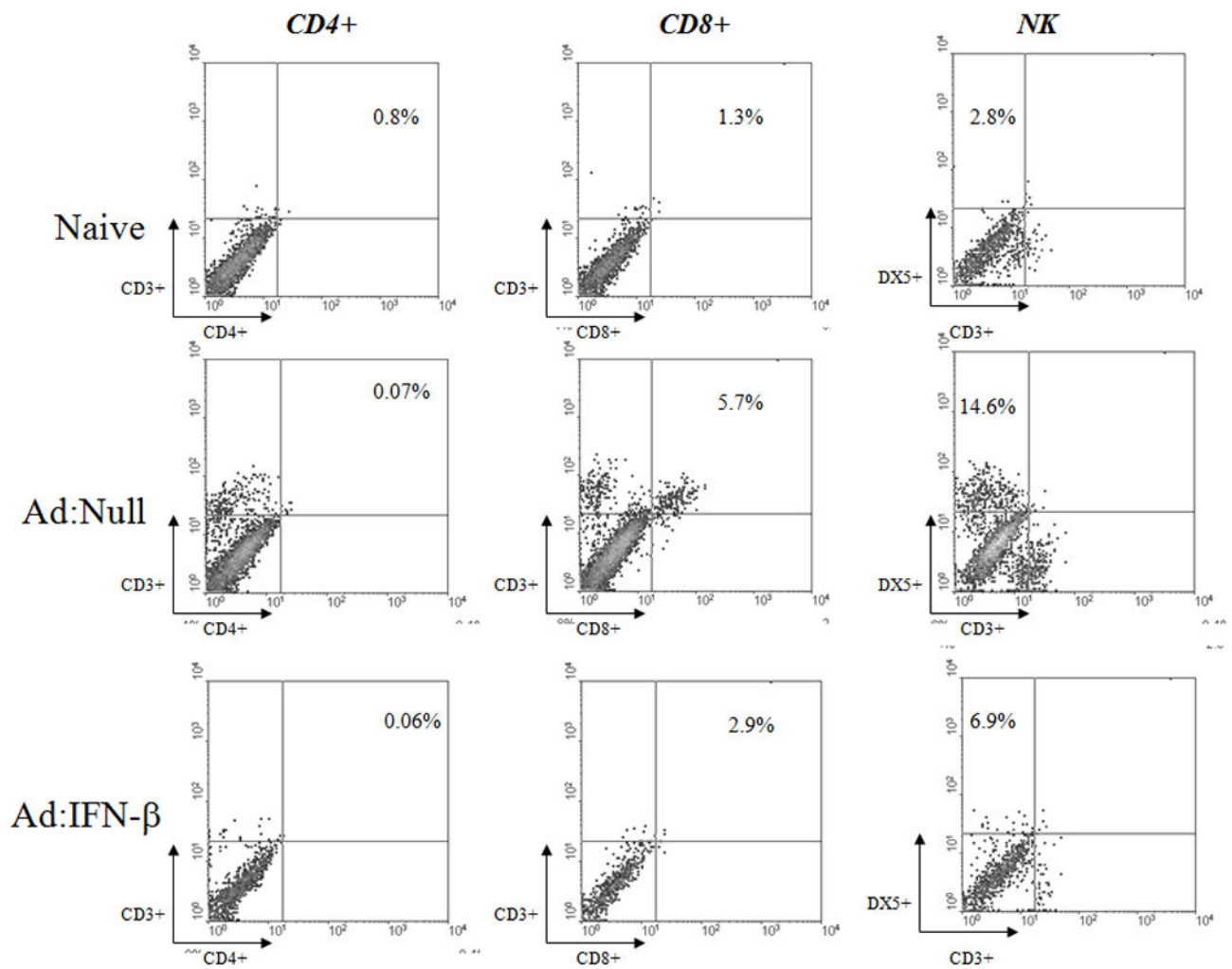
Figure 6. Ad:IFN-β transduction reduces lymphocyte infiltration in the TG of HSV-1 infected mice
Female C57BL/6 mice (n=4/group) were transduced with Ad Ad:IFN-β or Ad:Null vectors (1×10^6 transducing units/eye). Two days later, the mice were infected with HSV-1 (600 pfu/eye). Mice were euthanized 7 days post infection and the TGs were removed. TGs were collagenized and single cell suspensions were stained with the fluorochrome conjugated anti-CD4, anti-CD8α, anti-DX5, and anti-CD3 antibodies for 30 min at 4°C. The cells were analyzed on a FACS Calibur using WinMDI data analysis software.
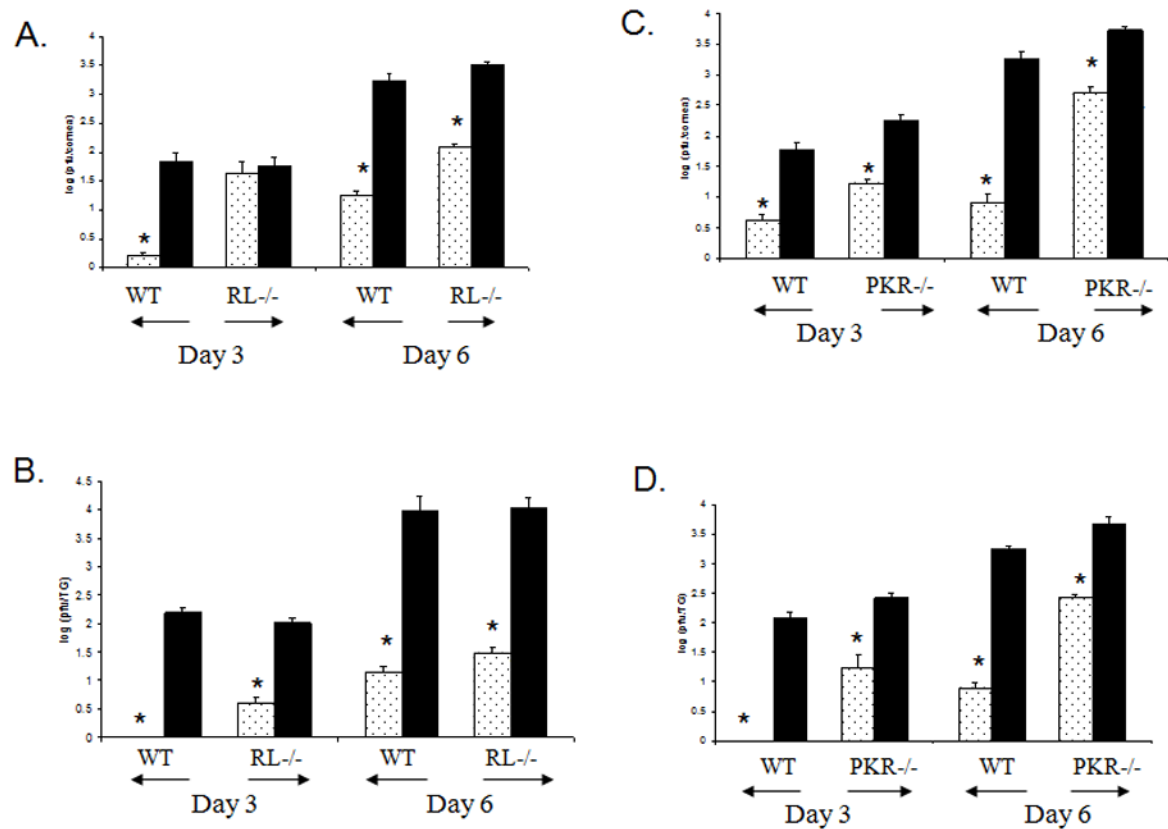
Figure 7. The absence of PKR reduces but does not eliminate the anti-viral action of the Ad:IFN-β vector against ocular HSV-1 infection while the absence of a functional OAS pathway transiently reduces the anti-viral efficacy of the Ad:IFN-β vector in the cornea

Wild type (WT) and mice deficient in RNase L (RL–/–) or PKR (PKR–/–) (n=4 per group/experiment) were transduced with Ad:IFN-β (dotted column) or Ad:Null vectors (black column) (1×10^6 transducing units/eye). Two days later, the mice were infected with HSV-1 (600 pfu/eye). Mice were euthanized 3 or 6 days post infection, and the cornea (A, C) and the TG (B, D) were removed. The tissue was homogenized and the clarified homogenate (10,000 × g, 1 min) was quantified for infectious virus by plaque assay. Results are a summary of three independent experiments. Bars represent the log of the mean +/− SEM. *$p<.05$ comparing the Ad:IFN-β to the Ad:Null treated mice.

Table I

Mice treated with Ad:IFN-β express lower IFN-γ levels and reduced CD8^{+} T lymphocyte and NK cell infiltration in the TG[a]

Treatment	NK^{+}CD3^{−}	CD4^{+}CD3^{+}	CD8^{+}CD3^{+}	IFN-γ protein[c]	IFN-γ transcripts[d]
None infected	2.42±0.2[b]	0.68±0.06	1.03±0.1	0	undetectable
Ad:Null	12.13±0.8[*]	0.67±0.05	4.98±0.3[*]	21±5.6[*]	4.3±1.2[*]
Ad:IFN-β	5.82±0.5[¶]	0.65±0.05	2.76±0.3[¶]	3±0.2[¶]	1.0±0.3[¶]

[a]Female C57BL/6 mice (n=4/group) were transduced with Ad:IFN-β or Ad:Null vectors (1×10^6 transducing units/eye). Two days later, the mice were infected with HSV-1 (600 pfu/eye). Mice were euthanized 7 days post infection and the TGs were removed. Single cell suspensions were prepared for flow cytometry. For purposes of ELISA, TGs were briefly homogenized and treated with a lysis buffer supplemented with a cocktail of EDTA-free protease inhibitors. Samples were then centrifuged and supernatants were assayed in triplicate. To measure transcript levels, RNA was isolated from the resected TGs and cDNA was subsequently synthesized. The relative gene expression was measured using a pre-developed IFN-γ specific TaqMan reagent (PE Biosystems, Forster City, CA). Results are a representative of two independent experiments (n=4 per group/experiment), except for the PCR experiment which was conducted once (n=4 per group).

[b]Numbers represent the percentage of cells present in the TG from the total number of gated cells ± SEM.

[c]Numbers represent the concentration of IFN-γ (pg/TG) ± SEM.

[d]Numbers represent the relative values of expression of IFN-γ transcripts normalized to GAPDH transcript values ± SEM.

[*]
$p < 0.05$ comparing Ad:Null transduced group to Ad:IFN-β transduced and to non-infected group.

[¶]$p < 0.05$ comparing Ad:IFN-β transduced group to non-transduced group.

Table II

Ad:IFN-β up-regulates OAS expression in the cornea and TG[a]

Tissue	Treatment	PKR[b]	OAS1a[b]
Cornea	Ad:IFN-β	1.8 ± 0.6	2.3 ± 0.4 [*]
	Ad:Null	0.9 ± 0.7	1.0 ± 0.2
	Vehicle	1.3 ± 0.2	1.0 ± 0.2
TG	Ad:IFN-β	1.5 ± 0.3	2.7 ± 1.1 [*]
	Ad:Null	0.7 ± 0.1	1.0 ± 0.2
	Vehicle	1.3 ± 0.2	1.0 ± 0.1

[a]Female ICR mice were treated with Ad:IFN-β, Ad:Null, or vehicle (PBS). Two days later, the mice were euthanized, and the cornea and the TG were removed. RNA was isolated and real time PCR was used to determine the relative gene expression. Results are a representative of two independent experiments (n=4 per group/experiment).

[b]Numbers represent the relative values of expression of viral gene transcripts normalized to GAPDH transcript values ± SEM.

[*]$p < 0.05$ comparing Ad:IFN-β transduced mice to Ad:Null transduced or to non-transduced animals.